Relevance of photocatalytic redox transformations of selected pharmaceuticals in a copper- and iron-rich Mediterranean intermittent river

M.V. Barbieri, Serge Chiron

Relevance of photocatalytic redox transformations of selected pharmaceuticals in a copper- and iron-rich Mediterranean intermittent river

Maria Vittoria Barbieri* and Serge Chiron

UMR HydroSciences Montpellier, University of Montpellier, IRD, CNRS, 15 Av. Charles Flahault 34093 Montpellier cedex 5, France.

*Corresponding author: maria-vittoria.barbieri@umontpellier.fr

Abstract

This work aimed at investigating specific attenuation pathways of pharmaceuticals in copper- and iron-rich Mediterranean intermittent and sunlit rivers by combining lab- and field-scale studies. Poorly photodegradable and biodegradable compounds such as fluconazole, oxazepam and venlafaxine attenuated in two river stretches with short hydraulic residence times (< 3 h). This result was assumed to be related to their capacity to interact with photoreactive free Cu^{2+} and Fe^{3+} or their associated oxides. Lab-scale photodegradation experiments under simulated solar irradiation revealed the beneficial impact of a mixture Cu^{2+} and colloidal iron hydroxides at environmental concentrations and at neutral pH on the pharmaceuticals photodegradation kinetic rate constants. These latter were consistent with the in-stream attenuation rate constants of targeted contaminants which ranged from 0.104 to 0.154 h^{-1}. Further identification of phototransformation products by LC-HRMS highlighted reductive transformation pathways including reductive dehalogenation and hydrogenation reactions. Several TPs were found to be stable under irradiation and were detected in field monitoring, accordingly. This was ascribed to the formation of a Cu/Fe composite material under solar irradiation with photocatalytic properties. The role of Cu was to trap the electron in the conduction band of the iron-based photocatalyst, which promoted separation efficiency of electron-hole pairs as well as enhanced photoreduction processes at the expense of oxidation ones. Even though, these mechanisms have been reported in water treatment field for organic micropollutants removal, their significance was demonstrated for the first time in natural settings.

Keywords: Copper; in-stream attenuation; pharmaceuticals, photocatalytic reductive reactions; transformation pathways.

1. Introduction

Attenuation of pharmaceutical mixture concentrations such as hydrochlorothiazide, valsartan and naproxen has mostly been studied in wastewater effluent-dominated perennial streams in temperate-regions and more scarcely in temporary rivers where increased pharmaceuticals concentrations could be observed due to the lack of dilution capacity (Mandaric et al., 2019). These studies were mainly conducted by using a combination of field studies and controlled laboratory experiments to investigate the attenuation dynamics and the associated predominant mechanisms of pharmaceutical dissipation along river stretches. A main outcome of these studies has been that variable pharmaceuticals inputs and differential in-stream attenuation generate evolving complex mixtures along stream reaches during base flow conditions with unpredictable impacts to biota (Zhi et al., 2020). Major factors affecting the extent of in-stream attenuation intensity of pharmaceuticals and their transformation products (TPs) including sorption, photo- and bio-transformations are still a matter of discussion (Jaeger et al., 2019). However, the relevance of each process is compound specific and the in-stream attenuation rate is highly variable among river segments (Acuna et al., 2014).

The primary mechanism for cationic pharmaceuticals attenuation (e.g., venlafaxine and citalopram) is thought to be sorption to sediment and biofilm (Writer et al., 2013) while for more polar and/or anionic compounds which are expected to remain in the water phase (e.g., diclofenac and hydrochlorothiazide) photodegradation may prevail (Schmitt et al., 2021). Biodegradation may become relevant providing that the hydraulic retention time is long enough, since increased water travel time accounts for higher attenuation of most of pharmaceuticals (Mandaric et al., 2019). This was demonstrated for instance for metoprolol by implementing an enantiomeric fractionation methodology (Kunkle and Radke, 2012). However, most current understanding of chemical attenuation mechanisms in aquatic systems comes from laboratory experiments, which do not cover

all the environmental conditions and can yield different transformation rates and TPs than real-world conditions.

A special case is undoubtedly Mediterranean intermittent streams because the Mediterranean hydrological regime is characterized by brief and intense flow events after dry periods of small streams. This implies an important physical erosion associated with copper and iron transfer to rivers by suspended matter in water runoff (Xue et al., 2000) leading to iron- and copper-rich river sediment. For instance, high Cu concentration levels could be determined in river-bed sediments of a small Mediterranean vineyard catchment (60 - 176 µg/g) together with a high content of Fe_2O_3 (5.4%) as well as in river suspended matter (146 - 191 µg/g), while dissolved Cu fraction of river waters could reach up to 8 µg/L (El Azzi et al., 2013). High levels of Cu has frequently originated from high repeated spraying of Bordeaux mixture (i.e., $Ca(OH)_2$ + $CuSO_4$) for crops protection against fungal diseases. Those streams also receive high amounts of organic matter from domestic wastewater treatment plants (WWTPs) and undergo changes in redox conditions, including from wet–dry cycles resulting from variable flow regimes. Consequently, dissolved Fe and Cu is produced through reductive dissolution of Cu oxides and Fe oxy(hydr)oxides, driven by microbial degradation of organic matter (Iles et al., 2022).

We hypothesized that Cu and Fe alone or as metal composite might contribute to the in-stream attenuation of organic micropollutants because Cu and Fe complexes with organic ligands including organic contaminants are photoreactive (Sykora, 1997) and because iron and copper oxides as solid or colloidal particles have shown photocatalytic activities (Asif et al., 2021; Sibhatu et al., 2022). Their photocatalytic properties have been deeply implemented in water treatment for organic micropollutants removal. In contrast, their relevance in natural waters has been poorly investigated. This will be the major contribution of this work by combining a field study during two months in the Crieulon and Vidourle River watersheds and controlled laboratory experiments as recommended (Zhi et al., 2021). The Crieulon River is a small Mediterranean intermittent stream, tributary of the

Vidourle river, with only one-point source of contamination (i.e., a psychiatric hospital effluent discharge), making it a near-ideal field site to study the attenuation behaviors of pharmaceutical mixtures (see a map in Fig. S1).

Specific objectives included (i) a monitoring study of selected pharmaceuticals along two river stretches using passive samplers, (ii) photodegradation kinetic experiments under simulated sunlight irradiation using Cu^{2+}/Fe^{3+} ions as well as different micrometric iron and copper oxides and spinel copper ferrite and (iii) TPs identification for selected compounds using liquid chromatography high resolution-mass spectrometry (LC-HRMS) for a deeper understanding of photodegradation mechanisms and their significance in investigated rivers. In this study, we will address and demonstrate the enhanced efficiency in photocatalytic oxidation/reduction of pharmaceuticals due to the formation of a Cu/Fe complex under solar irradiation for the first time in natural attenuation settings.

2. Materials and Methods

2.1 Chemicals

Analytical standards of targeted compounds atenolol, candesartan, carbamazepine, celiprolol, fluconazole, lamotrigine, oxazepam, sulpiride, tramadol, venlafaxine and their deuterated homologues, N,N-didesmethylvenlafaxine and venlafaxine-N-oxide were purchased from Toronto Research Chemicals (Toronto, Canada). Cetirizine, paroxetine and propanol were purchased from Sigma Aldrich (St Quentin-Fallavier, France). For extraction process and LC analysis, ultra-pure water (UPW) was obtained using a Millipore system; HPLC-grade acetonitrile (ACN) and methanol (MeOH) were purchased from Carlo Erba Reagents S.A.S. (Val de Reuil, France). Formic acid (FA) puriss p.a. ACS reagent analytical grade was purchased from Sigma-Aldrich (St Quentin-Fallavier, France). For the inorganic compounds, iron(II) oxide, iron(III) sulfate and spinel copper ferrite were purchased from Sigma-Aldrich (St Louis, USA). Copper(II) oxide was purchased from Alfa Aesar by Thermo Fischer Scientific (Ward Hill, USA), and copper(II) sulfate pentahydrate was purchased from Merck

KGA (Darmstadt, Germany). Humic acids sodium salt and ascorbic acid were purchased from Sigma-Aldrich (St Louis, USA).

2.2 Study site

Field surveys were conducted along two river stretches located in the northern part of Montpellier city (France). The first one of 1.7 km was selected on the Crieulon River with two sampling sites (SP1 and SP2, see Fig. S1) and the second one of 5.4 km on the Vidourle River with two sampling sites (SP3 and SP4). SP3 was located just after the confluence of the Crieulon River with the Vidourle River so that some dilution was expected. The Crieulon and the Vidourle are two small Mediterranean catchments, which were mainly occupied by vineyard, with a prolonged dry season and a mean annual average rainfall of 620 mm. The first stretch received water from one single continuous wastewater point-source from an effluent discharge of a psychiatric hospital (WWTP, SP1) while the second one received treated wastewater from different small villages located upstream to SP3. The WWTP outfalls were considered the principal sources of pharmaceuticals with minimal expected non-point source, representing a suitable study site for investigating the fate of these chemicals in surface water.

2.3 Sampling procedure

A tracer test was conducted the day before the sampling to estimate hydrologic travel times using fluorescent dye (rhodamine WT). Travel times from SP1 to SP2 and from SP3 to SP4 averaged 1.8 h and 2.6 h, respectively. River flow rates at the different SP were measured using an acoustic Doppler velocity meter (ADV; FlowTracker, SonTek, San Diego, CA, U.S.A.). The recorded values were 2.3, 2.3, 4.2 and 4.3 m^3s^{-1} at SP1, SP2, SP3 and SP4, respectively. Information on the quality of river waters at the 4 sampling points is reported in Table S1. High concentrations in dissolved Fe and Cu, in the 250 - 300 and 2 - 5 µg/L range, respectively, were the main feature of these waters (see Table 1). Polar organic chemical integrative samplers (POCIS) were used for environmental sampling because they have been demonstrated to be suitable to determine the attenuation of organic micropollutants in river and lead to similar results as those obtained through high-resolution sampling (e.g., Lagrangian

sampling scheme; Jaeger at al., 2019; Li et al., 2016). The targeted compounds concentrations in ng/L in river water were not needed for attenuation assessment because it was assumed that the uptake kinetics of a compound were identical along each river stretch, which was a reasonable assumption as the river characteristics did not change substantially between SP1 and SP2 as well as between SP3 and SP4. Consequently, the compounds amount was expressed in ng/g of dry POCIS sorbent. There was no field blank for POCIS, but the results from the procedural blank samples showed that there was no contamination during sample extraction and analysis.

Environmental sampling was carried out in June and July 2021 and POCIS were let for pharmaceuticals accumulation during three weeks. At each sampling site, one cage containing 3 POCIS discs was vertically submerged with a total sampling area of 41 cm^2. AttractSPE®POCIS HLB were purchased from Affinisep (Houlme en Normandie, France) consisting of approximately 230 mg of the solid adsorbent N-vinylpyrrolidone-divinylbenzene (Oasis HLB), which is a universal sorbent used to extract a wide range of compounds with a large range of polarity (Alvarez, 2010). During the sampling period, weather was mostly sunny with only two clouded days and no rain. In these conditions, solar radiation intensity ranged between 200 Wm^{-2} during clouded days to 1000 Wm^{-2} at midday during the sunny days.

Compounds attenuation rate constants k_{att} along the two river sections were determined assuming a first-order process from the slope of Eq. 1 ($Ln[C]t/[C]t_0 = k_{att} \times t$), with $[C]_0$ at the sampling sites 1 and 3 and $[C]_t$ at the respective downstream sites 2 and 4. The validity of this approach assumed no major dilution or input of the chemicals along the river sections and was tested under the conditions during our field study with carbamazepine, which is known as a conservative contaminant (Jaeger at al., 2019). Carbamazepine showed negligible attenuation along the two river stretches (see Table 1). Compounds k_{att} were determined based on a mean travel time of 1.8 h from SP1 to SP2 and 2.6 h from SP3 to SP4.

2.4 Photochemical studies

159 Photolysis of target compounds was carried out in parallel experiments in Pyrex glass cells with
160 distilled water spiked with 10 mg/L of each compound (direct photolysis) and with 10 mg/L of
161 micrometric iron oxide, copper oxide, spinel copper ferrite, Cu^{2+}, Fe^{3+}, and Cu^{2+}/Fe^{3+} mixture (in
162 separate experiments). In the Cu^{2+}/Fe^{3+} experiment, $[Cu^{2+}]$ and $[Fe^{3+}]$ was 10 µg/L each as well as the
163 concentrations of pharmaceuticals (10 µg/L) in presence of 10 mg/L of humic substances to better
164 reflect environmental conditions. The irradiation was performed using a 1500 W Xenon lamp
165 (Suntest, CO.FO.MEGRA, Italy) equipped with a 290 nm cut-off filter simulating solar light. The
166 irradiance was set at 750 W m^{-2} because in Montpellier area, in summer time (sampling period), solar
167 irradiance can reach 1000 Wm^{-2} at midday during a sunny day. The water temperature reached
168 during the irradiation was 55°C and the pH was adjusted in each experiment with the addition of
169 sodium hydroxide (NaOH) if necessary to remain constant at 7.5. This pH value was very close to the
170 ones of river water samples. A temperature of 55°C was not realistic but it is known that
171 photochemical kinetics do not significantly depend on temperature.

172 One mL of aliquots was collected at pre-determined intervals over the course of 24 h. The remaining
173 water at the end of each test was collected and the volume measured to determine loss via
174 evaporation for adjustment. Each experiment was conducted in triplicate and results were reported
175 as mean values. Iron and copper oxide dissolution with ascorbic acid was performed based on a
176 methodology proposed by Joseph et al. (1995) to confirm sorption processes of pharmaceuticals. All
177 samples were filtered through 0.45 µm syringe filters and directly analyzed by LC-HRMS for kinetic
178 studies and TPs identification. The phototransformation rate constants k_{photo} and related half-lives
179 ($T_{1/2}$) were determined analogously to Eq. 1 ($Ln[C]_t/[C]_{t0} = k_{photo} \times t$) with $[C]_t$ referring to
180 concentrations of compounds at each time point relative to the starting concentration $[C]_{t0}$.

181 2.5 Sample processing and analysis

182 *Target analysis:* Upon retrieval, POCIS discs were individually washed with distilled water, sealed in
183 its original aluminum bag, transported to the lab in ice box and stored under - 20°C until extraction.

Receiving phases of the POCIS were transferred into 3 mL empty polypropylene SPE cartridges, spiked with deuterated standards (1 mg/L acetonitrile), and then eluted with 8 mL of acetonitrile. After concentration under a gentle stream of nitrogen, final extracts (1.5 mL) were analyzed by LC-HRMS. The chromatographic run was carried out by means of Dionex™ Ultimate 3000 UHPLC (Thermo Scientific™, San Jose, USA) using a Waters XBridge C_{18} column (150 x 2.1 mm i.d., 2.5 µm particle size). The mobile phases were 0.1% FA in water (A) and 0.1% FA in MeOH (B) under the following gradient: 95%A:5%B from 0 to 1 min, 90% B at 19 min with a 1 min hold, 5% B at 20.5 min, followed by a 5 min equilibration at 95%A:5%B. The flow rate was 0.3 mL/min. The MS analysis was performed with an Q-Exactive™ Focus Orbitrap mass spectrometer (Thermo Fisher Scientific, Les Ullis, France) equipped with an HESI electrospray source and operated in positive ionization mode in full scan acquisition. Further details of MS and HESI parameters are provided in SM. For the quantification of targeted pharmaceuticals, matrix calibration curves were made according to the matrix match standard procedure using the internal standard method (European Commission, 2017). Analytical limits of detection (LODs) and limits of quantifications (LOQs), as well as linearity, accuracy and precision of the method have been previously validated in our group and reported in Tadić et al. (2022).

Non-target analysis: Samples were analyzed using a Vanquish ultra-high performance liquid chromatography (Thermo, Fisher Scientific, Waltham, MA, USA) coupled to a high-resolution mass spectrometry Q-Focus Orbitrap (Thermo Fisher Scientific, Waltham, MA, USA) equipped with a heated electrospray ionization (HESI) source operated in full scan + data dependent acquisition MS2 (DDA-MS2) mode. The chromatography assay was performed using 10 µL injection volume, 0.3 mL/min flow rate, and a binary gradient of water (A) and acetonitrile (B), both containing 0.1% formic acid, as follows: 10% B at 0–1 min, 90% B at 10–20 min, 10% B at 21–27 min. Data were treated using Thermo Xcalibur™ 3.1 Software (Thermo Fisher Scientific, CA, USA). The specific workflow and instrumental conditions used for elucidating transformation products is provided in SM.

209 **Table 1**. Concentrations in ng/g of POCIS sorbent ± relative standard deviation (RSD) for targeted
210 pharmaceuticals and in μg/L for dissolved Cu and Fe at four sampling sites (SP1, SP2, SP3 and SP4)
211 along the investigated river stretch during June and July 2021. See the map in Supporting Material for
212 sampling sites location.

Compound	SP1	SP2	SP3	SP4
		June 2021		
Sulpiride	<LOQ	<LOQ	1.9 ± 0.4	1.6 ± 0.35
Atenolol	<LOQ	<LOQ	2.3 ± 0.3	0.8 ± 0.1
Tramadol	43.8 ± 5.3	34.3 ± 4.1	27.0 ± 3.2	23.4 ± 2.8
Fluconazole	379.2 ± 45.5	265.7 ± 29.5	172.3 ± 20.7	103.8 ± 12.5
Lamotrigine	348.5 ± 38.3	326.5 ± 35.9	56.8 ± 6.2	61.4 ± 6.8
Celiprolol	20.7 ± 1.7	14.7 ± 1.2	37.3 ± 3.0	15.2 ± 1.2
Venlafaxine	175.5 ± 14.0	129.3 ± 10.3	59.2 ± 4.7	36.8 ± 2.9
Propanolol	7.8 ± 0.5	6.7 ± 0.4	143.4 ± 8.6	66.2 ± 4.0
Paroxetine	6004.7 ± 420.3	3766.5 ± 263.7	1932.2 ± 135.3	730.9 ± 51.2
Cetirizine	8.7 ± 1.2	4.7 ± 0.7	7.2 ± 1.0	5.8 ± 0.8
Oxazepam	12244.5 ± 979.6	8948.3 ± 795.9	3199.3 ± 255.9	1632.3 ± 130.6
Candesartan	2.1 ± 0.2	2.9 ± 0.2	5.3 ± 0.4	4.6 ± 0.4
Carbamazepine	224.6 ± 11.2	232.7 ± 11.6	188.4 ± 9.4	182.6 ± 9.1
Soluble Cu	4.834 ± 0.145	3.679 ± 0.110	5.745 ± 0.172	2.265 ± 0.098
Soluble Fe	255.4 ± 10.2	324.2 ± 13.0	288.3 ± 11.5	312.5 ± 12.5
		July 2021		
Sulpiride	<LOQ	<LOQ	4.0 ± 0.9	3.6 ± 0.8
Atenolol	<LOQ	<LOQ	1.7 ± 0.2	<LOQ
Tramadol	12.6 ± 1.5	10 .3 ± 1.2	178.6 ± 21.4	156.7 ± 18.8
Fluconazole	280.4 ± 22.4	221.7 ± 17.7	132.6 ± 10 .6	85.4 ± 6.8
Lamotrigine	245.6 ± 27.0	224.2 ± 24.7	76.8 ± 8.4	65.6 ± 7.2
Celiprolol	24.5 ± 2.0	18.4 ± 1.5	61.9 ± 5.0	19.4 ± 1.6
Venlafaxine	145.6 ± 11.6	110.6 ± 8.8	48.7 ± 3.9	32.4 ± 2.6
Propanolol	<LOQ	<LOQ	4.9 ± 0.3	<LOQ
Paroxetine	4564.8 ± 319.6	3067.3 ± 214.7	2568.2 ± 179.8	1120.5 ± 78.4
Cetirizine	6.4 ± 0.9	5.3 ± 0.7	9.2 ± 1.3	8.5 ± 1.2
Oxazepam	8934.6 ± 714.8	5896.4 ± 471.7	2435.8 ± 194.9	1296.6 ± 103.7
Candesartan	2.6 ± 0 .2	2.2 ± 0.2	37.5 ± 3.0	35.8 ± 2.9
Carbamazepine	318.7 ± 15.9	312.3 ± 15.6	247.4 ± 12.4	236.9 ± 11.8
Soluble Cu	4.245 ± 0.127	3.456 ± 0.104	5.423 ± 0.163	2.867 ± 0.086
Soluble Fe	232.4 ± 9.9	312.2 ± 12.5	284.3 ± 11.4	308.5 ± 12.3

213

214 3. Results and discussion

215 3.1 Occurrence and attenuation of targeted pharmaceuticals along two river stretches

216 For pharmaceuticals monitoring, a first LC-HRMS-based non-target screening workflow was
217 implemented for the identification of 47 pharmaceuticals in river water samples (Tadić et al., 2022)
218 of which 13 compounds were commonly quantified in POCIS extracts mainly including β-blockers (3),
219 and psychiatric drugs (6) (see Table 1). The most persistent compounds were tramadol, lamotrigine,

sulpiride, candesartan and carbamazepine while the other ones including atenolol, celiprolol, fluconazole, venlafaxine, propranolol, paroxetine, and oxazepam underwent dissipation to different extents along the river reaches. To check for hydraulic dilution, a conservative tracer (i.e., carbamazepine) was used. Carbamazepine concentrations remained stable between sampling sites SP1 and SP2 as well as between SP3 and SP4 (see Table 1). Consequently, a decrease in concentrations between two consecutive sampling sites could only be ascribed to sorption, photo- and/or biotransformation processes and not to dilution. The riverbeds consisted mainly of gravel and sand with a lack of macrophytes so that absorption of contaminants by plants could be ruled out. However, their absorption by microorganisms and algae was likely to occur.

To gain evidence if biotransformation has occurred, the potential enantiomeric fractionation (EF) for chiral pharmaceuticals has been applied (Mechelke et al., 2020). Venlafaxine was selected for this purpose because biotransformation has been reported as an important in-stream attenuation process for venlafaxine (Schmitt et al., 2021). EF between SP1 and SP2 and between SP3 and SP4 were determined for selected samples with chiral chromatography following a methodology previously established by our group (Li et al., 2013). No significant change in EF was observed (see Fig. S2). EF is known to be strongly dependent on environmental conditions (e.g., microbial communities, Mechelke at al., 2020) most likely accounting for discrepancies between the results of this study and those reported by Schmitt et al. (2021). The absence of EF of venlafaxine could not fully exclude biotic processes for other compounds because potentially different enzymes are responsible for the transformation of different drug families. However, biotransformation could be reasonably discarded as significant dissipation pathways at least for poorly biodegradable compounds such as fluconazole and oxazepam (Pacholak et al., 2022; Redshaw et al., 2008).

Sorption to sediment and photodegradation were very likely the two major processes accounting for pharmaceuticals attenuation. The behavior of some compounds was anticipated such as that of paroxetine due to quick direct and indirect photolysis (Gornick et al., 2021) and that of venlafaxine

and β blockers through sorption to sediment because they are positively charged at environmental pH facilitating interaction with negative surfaces of sediment (Li et al., 2015). To confirm this assumption, analysis of sediment samples was performed for selected compounds (see analytical methodology and results in Table S2 and S3).

Lamotrigine, tramadol, celiprolol, venlafaxine, propanolol and citalopram, which are basic drugs and positively charged at neutral pH were all quantified at a few ng/g levels. Oxazepam, a neutral compound but with a log K_{ow} = 2.2 was also detected in the 5 - 7 ng/g range while fluconazole, another neutral compound but with a lower K_{ow} = 0.5, was never detected. The fast attenuation of fluconazole was unexpected because this latter has frequently been used as a conservative tracer in in-stream attenuation studies due to its known high stability under photolysis and under biodegradation (Li et al., 2015) and lack of affinity for sediment. Fluconazole quickly dissipated with a mean attenuation rate constants (k_{att}) of 0.1 h^{-1} over the two sampling campaigns in June and July, assuming a pseudo first-order reaction (see experimental section). However, dissolved Fe and Cu heavily occurred in the investigated waters with concentrations in the 2.3 - 5.7 and 255.4 – 324.2 µg/L range, respectively as well as in river sediments (see Table 1). Fluconazole is known for its capacity to form complexes with transition metals such as Fe and Cu (Stevanović et al., 2021). Consequently, these two transition metals were assumed to play a role in fluconazole in-stream attenuation rates due to the potential photoreactivity of such complexes. This might hold true for oxazepam (Correira dos Santos et al., 2002) and venlafaxine (Alturiqui, 2018). In spite of some sorption to sediment, their fast dissipation rates were not anticipated since oxazepam and venlafaxine are not fast photodegradable compounds, with half-lives reported to be 66 and 58 h (West and Rowland, 2012; Manasfi et al., 2022). In contrast, lamotrigine is not known to undergo complexation with transition metals which might account for its persistence. Tramadol has been reported to form complexes with Cu but remained stable. However, the stability constant of tramadol complex with Cu (log β = 4.0, Mansoor and Farooqui, 2017) is less than half that of venlafaxine (log β = 9.6, Alturiqi et al., 2018). To confirm the assumption of the involvement of Cu

271 and/or Fe in the dissipation of selected compounds, lab-scale photodegradation experiments were
272 conducted.

273 3.2 Photodegradation of selected pharmaceuticals under controlled lab conditions

274 Lab-scale experiments were conducted to study phototransformation separately from other
275 processes (i.e., biotransformation and sorption) for a better understanding of in-stream attenuation
276 mechanisms of selected compounds. For this purpose, three pharmaceuticals, i.e., oxazepam,
277 venlafaxine and fluconazole were selected according to (i) their high occurrence in the investigated
278 river samples, as well as (ii) their known slow direct photodegradation kinetics and (iii) their tendency
279 to form complexes with transition metals (e.g., Cu(II) and/or Fe(II)). Fig. 1 shows photodegradation
280 kinetics under different conditions using dissolved Cu^{2+} and Fe^{3+} for their potential ability to form
281 complexes with targeted compounds, and Fe_2O_3 (hematite), CuO and spinel copper ferrite for their
282 photocatalytic behavior (Fig. 1a-c). Experiments with equal amounts of $Cu^{2+}$and Fe^{3+} (i.e., 10 µg/L)
283 were also carried out in presence of humic substances to better reflect environmental conditions
284 (Fig. 1d).

285

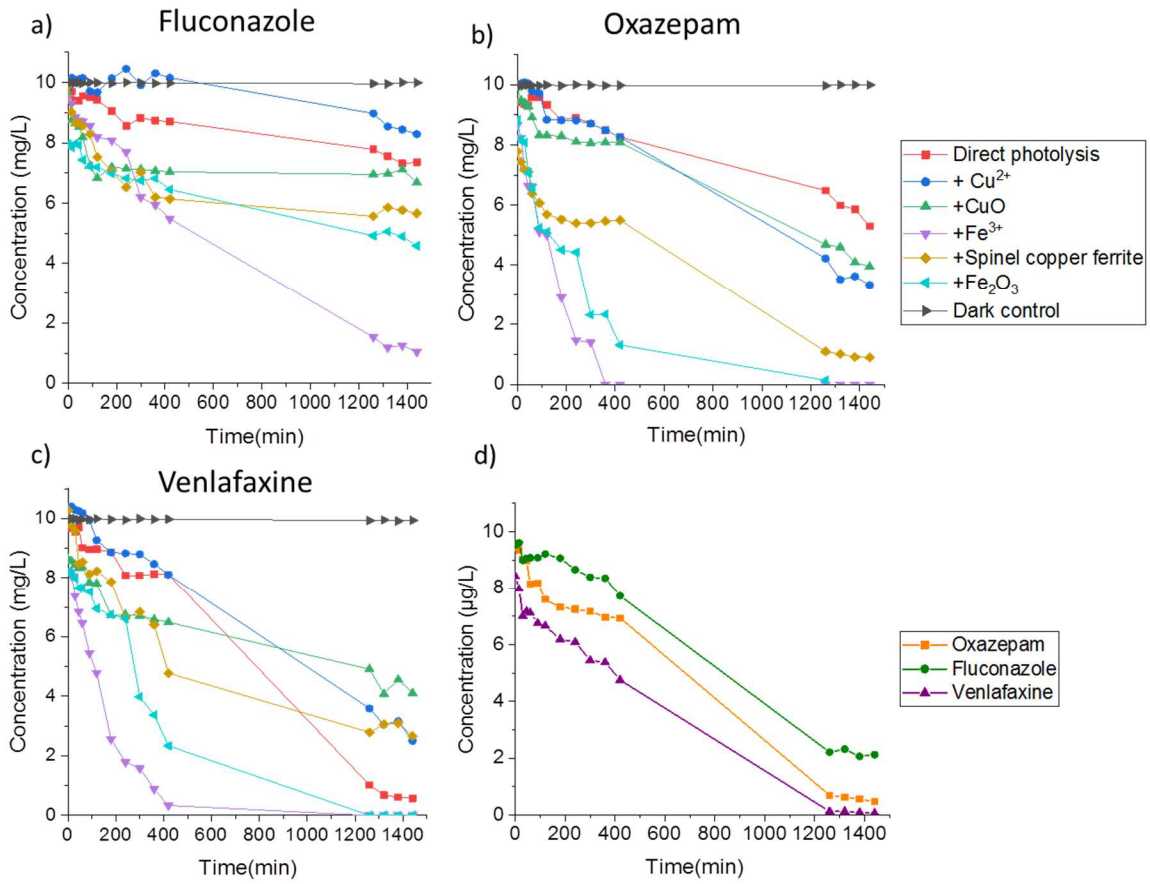

286

287 **Fig. 1.** Photodegradation of oxazepam (a), fluconazole (b) and venlafaxine (c) spiked at 10 mg/L, and
288 10 mg/L of iron oxide, copper oxide, Cu^{2+}, Fe^{3+}, spinel copper ferrite, and (d) a detail of
289 photodegradation kinetics of the three compounds at environmental concentrations (10 µg/L) in
290 presence of Cu^{2+} and Fe^{3+} ions mixture at 10 µg/L, with the addition of 10 mg/L humic acid.

291

292 No significant losses of oxazepam, venlafaxine or fluconazole were observed in the dark controls,
293 eliminating the possibility of thermal or hydrolytic degradation. Sorption processes of
294 pharmaceuticals mainly occurred with iron and copper oxides and colloidal iron hydroxides particles
295 resulting from the poor solubility of Fe^{3+} at neutral pH occurred at T_0. This was confirmed by iron and
296 copper oxide dissolution (see experimental section), which prompted the release of the sorbed
297 fraction excluding others abiotic transformation pathways than the photochemical one. Results
298 obtained under direct photolysis were consistent with those reported in literature, that is slow
299 degradation kinetic rates for oxazepam and fluconazole and faster ones for venlafaxine (Rua-Gomez
300 and Püttmann, 2013; Castro et al., 2016; Calisto et al., 2011).

301 The photodegradation of each compound followed rather well apparent first order kinetics ($r^2 > 0.98$)
302 under different conditions and the related kinetic rate constants (k_{photo}) and half-lives ($T_{1/2}$) were
303 calculated accordingly (see Table S4). The photodegradation kinetics were always faster with iron
304 than with copper. The generation of hydroxyl radicals under the photolysis of the colloidal ferric
305 hydroxide particles or under hematite photocatalytic activity most likely accounted for this result
306 (Sun et al., 2014). The potential complexation of pharmaceutical with Cu^{2+} did not result in significant
307 photodegradation kinetics enhancement (in comparison to direct phototransformation) and even in
308 deceleration in case of fluconazole and venlafaxine most likely due to light screening. This is in
309 contrast with cephalosphorines β-lactam antibiotics that underwent fast photodegradation in
310 presence of Cu^{2+} but in this case, a photoinduced hydrolysis of the lactam ring could explain the fast
311 photoreactivity (Zhang et al., 2020).

312 When Cu^{2+} was added to Fe^{3+} aqueous solutions at environmental concentrations, an increase in
313 k_{photo} was observed for the three target compounds (see Fig. 1d and Table S4). In this specific case,
314 the values of $T_{1/2}$ in lab and field studies agreed reasonably well considering the complexity of the
315 investigated field system and the assumptions that were made (e.g., constant mean travel time for
316 the whole sampling period). This holds particularly true for oxazepam with average $T_{1/2}$ of 4.5 and 5.5
317 h in the field and lab study, respectively (see Fig. 2).

318

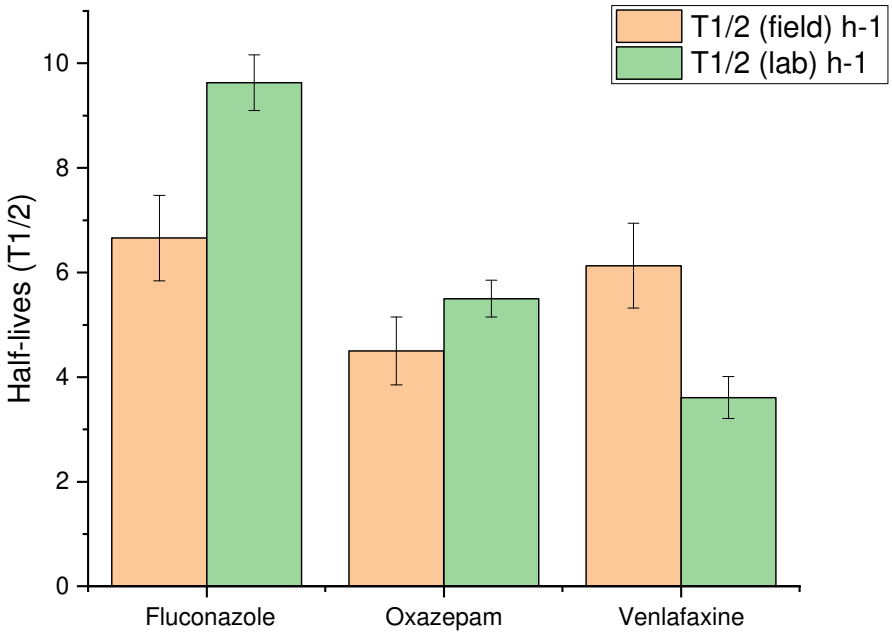

319

320 **Fig. 2**. Comparison of half-lives ($T_{1/2}$) of targeted compounds in field and lab-studies under photolysis
321 in distilled water with 10 µg/L Cu^{2+} and Fe^{3+}.

322

323 Higher $T_{1/2}$ values in the field than in the lab for venlafaxine might be attributed to partial adsorption
324 to the sediment, the adsorbed fraction becoming less accessible to solar irradiation. Indirect
325 photolysis of venlafaxine in river was likely to occur which has mainly been attributed to the
326 formation of hydroxyl radicals (Rua-Gomez and Püttmann, 2013), contrary to oxazepam and
327 fluconazole for which indirect photolysis was found insignificant (Calisto et al., 2011 ; Castro et al.,
328 2016). This meant that in presence of Cu^{2+} and Fe^{3+}, this pathway is likely becoming negligible. Lower
329 $T_{1/2}$ in the field than in the lab might be related to the insignificance of direct photolysis of
330 fluconazole. The photocatalytic property of iron oxy(hydr)oxides is limited due to the fast
331 recombination of electron-hole pairs. However, this photocatalytic activity in visible light is usually
332 enhanced in the presence of transitional metals such as Cu^{2+}. The role of this latter species is to trap
333 the electron in the conduction band of the photocatalyst, which promotes separation efficiency of

electron-hole pairs as well as enhances photoreduction processes (e.g., dehalogenation) at the expense of oxidation ones (Baumanis et al., 2011 ; Lei et al., 2016). However, this shift in contaminant transformation pathways, if rather known in water treatment settings, has not been demonstrated in natural attenuation settings. Photocatalysis is an interfacial reaction in which pollutants will be degraded more efficiently when they diffuse to the surface of the catalysts. Several studies have therefore shown that the synergy of adsorption and photocatalysis can efficiently enhance the pollutants removal rates (Yu et al., 2021). The affinity of Cu and Fe to bind with investigated pharmaceuticals might account for the observed enhanced efficiency in their photocatalytic oxidation/reduction.

3.3 Identification of TPs in lab-scale experiments and their occurrence in river water

For a possible elucidation of the mechanisms of phototransformation of targeted compounds, we proceeded to TPs identification under different experimental conditions using suspect and non-target LC-HRMS screening.

For venlafaxine, a total of nine TPs were identified. N,N-didesmethylvenlafaxine and venlafaxine-N-oxide were confirmed by comparison of the mass spectra and retention times to those of purchased synthetic compounds. Two TPs were identified by comparison with literature spectra (TPven-294 and TPven-292, Osawa et al., 2019). Five TPs were detected for the first time, the structures of which were assigned by interpreting MS data (see Fig. S3 for extracted ion chromatograms (EIC) and MS^2 spectra), mass accuracy, retention time plausibility, fragments ions, and on the basis of reactivity knowledge.

As a matter of example, in Fig. 3 the fragmentation pathway of TPven-251 is proposed. First, TPven251 has an even Mw indicating the loss of the nitrogen atom from venlafaxine structure. The MS^2 spectrum shows two major fragment ion at m/z 152.0467 and 163.0752. These ions were characteristic of cyclohexanol ring losses and the experimental masses at 152.0467 and 163.0752

could only match to $C_9O_2H_{12}$ and $C_{10}H_{11}O_2$ elemental composition, respectively, supporting the formation of a primary alcohol functional group.

TPven-249, TPven-251 and TPven-219 most likely arose from a one-electron oxidation at the C in position α of the secondary amine moiety leading to an unstable radical species. Even M_W of these TPs suggested N losses. Consequently, this unstable radical could evolve in different paths, including i) oxidation into an aldehyde following the formation of a hydroperoxyl radical in presence of O_2 (TPven-249), ii) reduction into the corresponding primary alcohol (TPven-251) and iii) neutralization by dehydration and rearrangement (TPven-219). DBE values of TPven-251 (4.5) and TPven-253 (3.5) differed in one unit, suggesting that TPven-253 most likely resulted from hydrogenation reaction (1 x2H) at the aromatic ring. An additional TP was detected at m/z $[M+H]^+$ = 282.2790. DBE value of this TP (2.5) was two units lower than that of venlafaxine (4.5) and hydrogenation reactions (2 x 2H) at the venlafaxine benzene ring was assumed to lead to TPven-282 (see Table S5 for MS data and proposed data and Fig. S3 for EIC and MS^2 spectra). No structure could be definitively assigned to TPven-279.

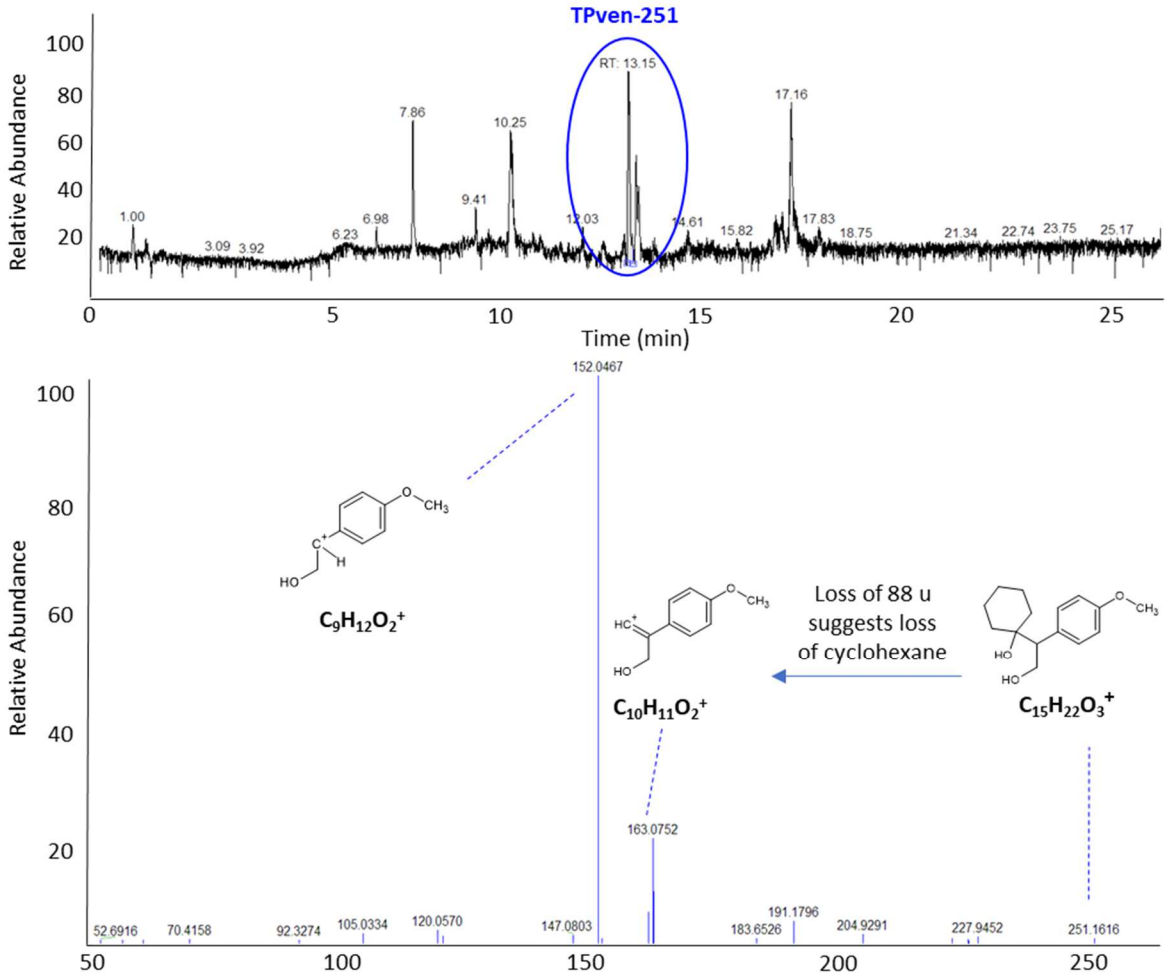

372

373 **Fig. 3.** Total Ion Chromatogram (TIC) with mass spectral peaks belonging to TPs from photolysis
374 experiments with a detail of TPven-251 peak at RT= 13.15, and ESI full scan mass spectra (m/z 50-
375 250) of degradation product TPven-251 with relative molecular ions and proposed fragmentation
376 pathway.

377

378 In the case of oxazepam, a total of five TPs were identified by comparison of literature spectra (Yang
379 et al., 2018; West and Rowland, 2012) including TPoxa-257, TPoxa-241, TPoxa-273, TPoxa-223 and
380 TPoxa-301 and two TPs remained unknown including TPoxa-227 and TPoxa-327 (see Table S5 for
381 experimental $[M+H]^+$ accurate M_W, possible elemental composition, together with mass error and
382 double bond equivalents (DBE) and proposed structures). The photodegradation pathway under
383 direct photolysis (blue arrow) was consistent with that previously reported with the formation of
384 quinazoline (TPoxa-241) and quinazolinone (TPoxa-257) derivatives. The phototransformation
385 pathway under Fe^{3+} irradiation (green arrow) involved oxidation reactions through hydroxylation

(TPoxa-273 and TPoxa-301) while Cu^{2+}/Fe^{3+} irradiation (orange arrow) accounted for a specific reduction reaction through reductive dechlorination leading to TPoxa-223.

Regarding fluconazole, five TPs were detected. The structures of TPflu-287 and TPflu-305 were confirmed thanks to the availability of literature spectra (Castro et al., 2016). Fluconazole dehydration (- H_2O) likely accounted for TPflu-289 formation. TPflu-301 and TPflu-317 were detected for the first time to the better of our knowledge. Their EIC together with their MS^2 spectra are shown in Fig. S3. As an aryl halide, TPflu-305 could undergo a radical-nucleophilic aromatic substitution through an aryl radical intermediary species following fluorine ion losses (Castro et al., 2016). This latter radical located in (m) position with respect to OH substituent shifted to (p) position by resonance accounting for the quinone formation (TPflu-301). TPflu-301 could evolve into TPflu-317 by further hydroxylation. The chemical structures of TPflu-269 and TPflu-257 could not be elucidated. On the basis of TPs identification, the suggested photodegradation fates of oxazepam, venlafaxine and fluconazole under different experimental conditions (i.e, direct photolysis, in presence of Fe^{3+} alone or a mixture of Fe^{3+}/Cu^{2+}) are presented in Fig. 4a, 4b and 4c, respectively.

a)

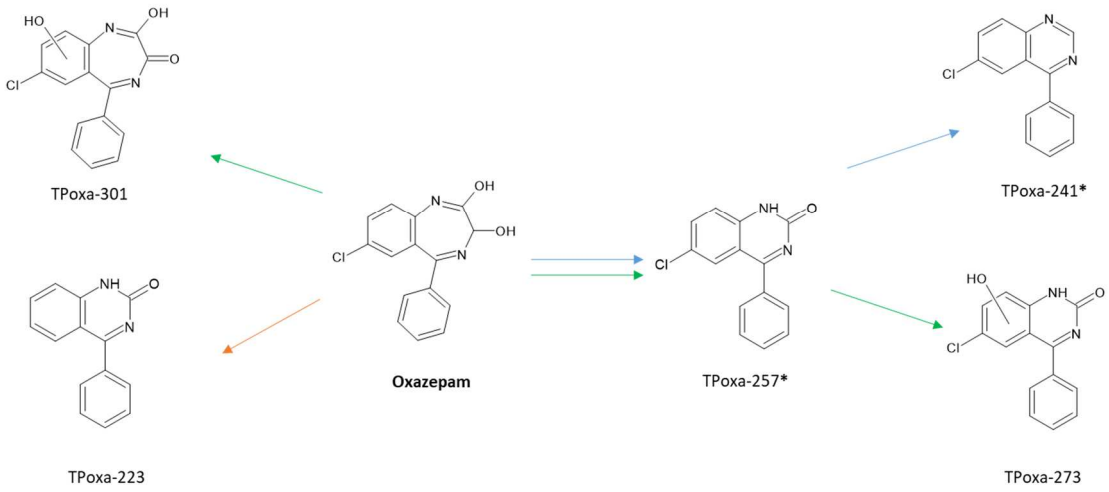

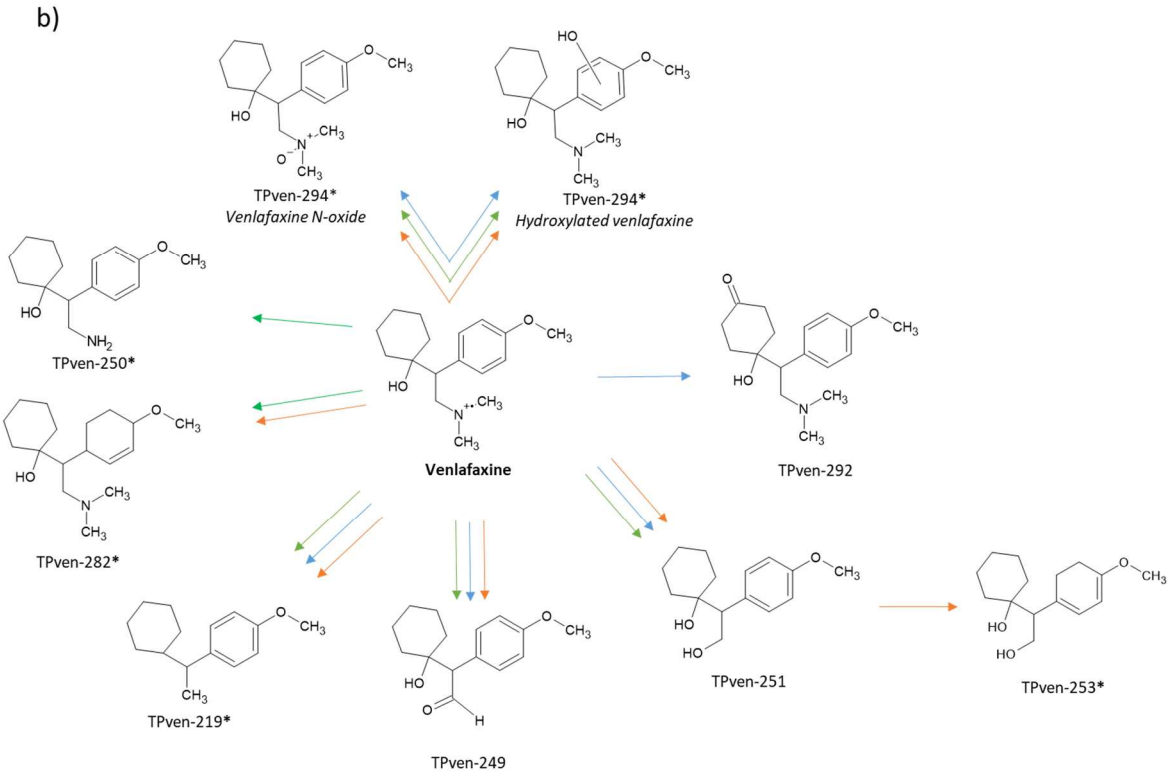

401

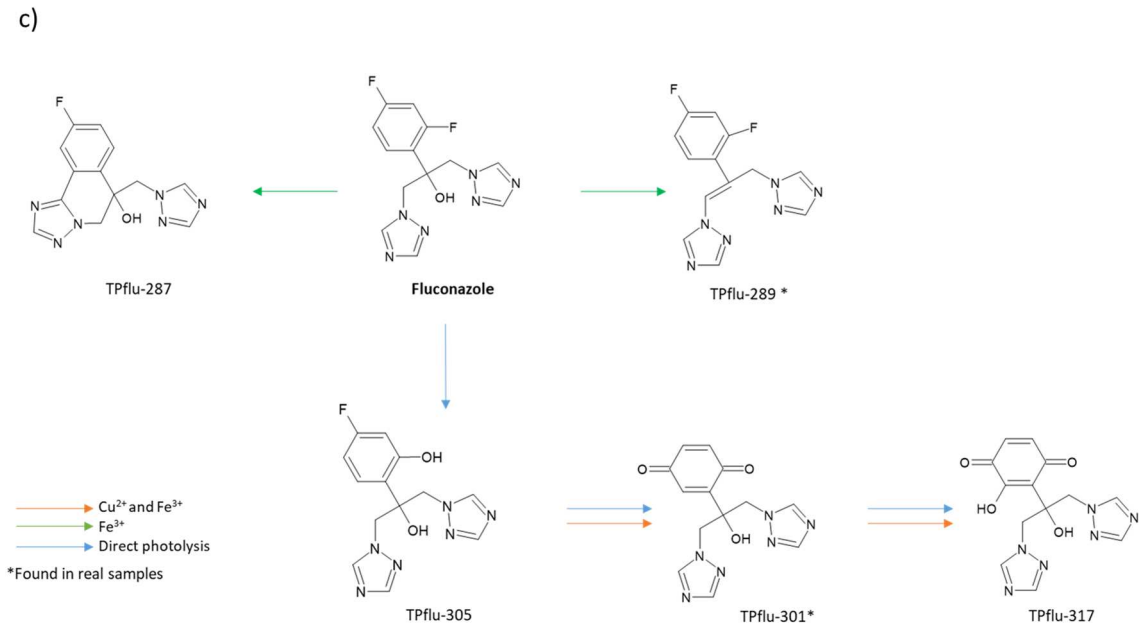

402

403 **Fig. 4.** Proposed photodegradation pathways of oxazepam, venlafaxine and fluconazole under (a)
404 direct photolysis (blue arrows), (b) in presence of Fe^{3+} (green arrows) and (c) Fe^{3+} with Cu^{2+} (orange
405 arrrows).
406 * compounds found in real samples.

407

408 As far as the venlafaxine photodegradation pathway is concerned, the competition between

409 oxidative and reductive pathways was not so noticeable between Fe^{3+} and Cu^{2+}/Fe^{3+} systems.

However, Fe^{3+} system appeared more oxidative than Cu^{2+}/Fe^{3+} system since N-dealkylation reactions leading to the formation of N, N-didesmethylvenlafaxine could be specifically attributed to Fe irradiation while Cu^{2+}/Fe^{3+} irradiation was responsible for hydrogenation reaction leading to the conversion of TPven-251 into TPven-253 and the conversion of venlafaxine into TPven-282. A common path between direct photolysis and the Fe^{3+} and Cu^{2+}/Fe^{3+} systems, initiated by a one-electron oxidation reaction at the C located in α position of the N atom was also observed. This reaction was enabled because the resulting radical was stabilized by resonance and could be further reduced, oxidized or neutralized to give TPven-219, TPven-249 and TPven-251. Other already known direct photodegradation pathways involved the formation of N-oxidized, hydroxylated (TPven-294) and ketone (TPven-292) derivatives.

Regarding fluconazole, the formation of TPflu-305 and TPflu-301 went through radical-nucleophilic substitutions of fluorine atoms. This is a reduction reaction with the formation of a radical anion as intermediary species. Fluorine is known to be a better leaving group than chlorine and defluorination could therefore also occur under direct photolysis. Why this substitution reaction did not proceed in Fe^{3+} system was not elucidated. In contrast, Fe^{3+} system led to a cyclisation reaction rather than the substitution reaction after the formation of the radical anion as well as to venlafaxine dehydration. The evolution of TPs abundances against time was followed on the basis of peak area to anticipate which TPs may accumulate in Cu^{2+}/Fe^{3+} system (see Fig. 5).

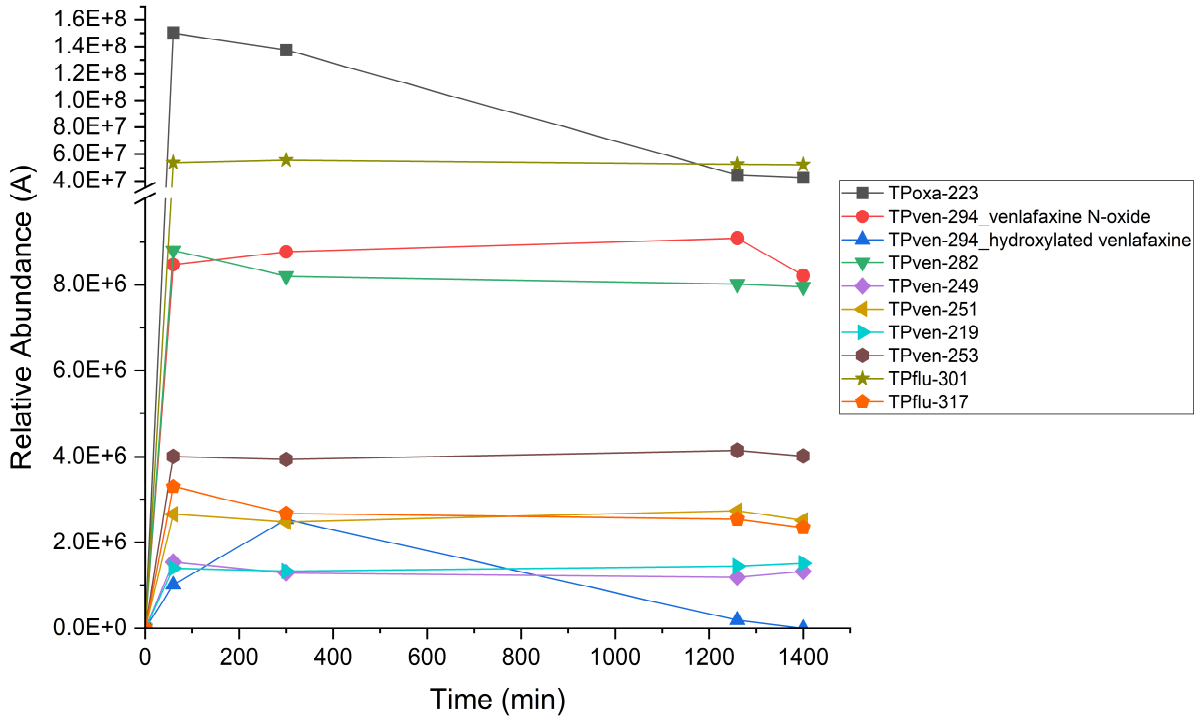

Fig. 5. Evolution of TPs concentrations expressed in relative peak abundance against time after Cu^{2+}/Fe^{3+} irradiation at environmental conditions (i.e. Cu^{2+}/Fe^{3+} at 10 µg/L with the addition of 10 mg/L humic acid).

All significant TPs were quickly formed during the first 60 min of irradiation and later on reached steady-state concentrations (i.e., formation and degradation offset one another) with the exception of hydroxyl-venlafaxine TP and TPoxa-223 which slowly underwent further degradation. This 1 h time frame of formation was compatible with TPs in-stream formation since HRTs were higher than 1 h and was consistent with the detection of a few of these TPs in field monitoring including TPoxa-257, TPoxa-241, venlafaxine-N-oxide, N,N-didesmethylvenlafaxine, hydroxy-venlafaxine, TPven-282, TPven-250, TPven-219, TPven-253, TPflu-289 and TPflu-301. Interestingly, while venlafaxine-N-oxide, hydroxyl-venlafaxine and N,N-didesmethylvenlafaxine already occurred in the hospital WWTP discharges (Manasfi et al., 2022), the other detected TPs were in-stream generated, highlighting the relevance of photocatalytic redox processes in sunlit river, especially reductive dehalogenation or hydrogenation reactions with the detection of TPven-282, TPven-253 and TPflu-301.

Co-catalyst-assisted photocatalytic reduction have been widely demonstrated using for instance Rh-loaded TiO_2 for hydrogenation of aromatic ring (Nakanishi et al., 2018) or CuO-modified TiO_2 nanocomposites for dehalogenation of polybrominated diphenyl ethers (Lei et al., 2016). In this latter system, the supposed mechanism involved CuO trapped electrons from visible light irradiated TiO_2 to form Cu_2O. The higher reduction potential of Cu_2O over CuO and TiO_2 allows for transferring electrons to contaminants initiating the photocatalytic process. Similar behavior in the Cu^{2+}/Fe^{3+} system might be anticipated where in irradiated solutions Cu^{2+} might be bound to the surface of the hydrous iron oxide and/or CuO might precipitate at the surface of the oxide (Boukhalfaa et al., 2010). This system to be effective required compound adsorption / complexation at the catalyst surface. This explained what it only worked for those pharmaceuticals (i.e., fluconazole, oxazepam and venlafaxine) which can form complexes with transition metals such as Cu and Fe. The characterization of the metal composite material generated under Cu^{2+}/Fe^{3+} irradiation and its interaction with pharmaceuticals was outside the scope of this work but would deserve further investigation.

4. Conclusions

This study investigated the fate of selected pharmaceuticals in Cu- and Fe-rich waters of twoMediterranean intermittent rivers at lab- and field-scale. It is often challenging to transfer kinetics from the laboratory to complex variable field conditions. However, in this study, only photochemical processes due to Cu and Fe photoreactivity accounted for attenuation of investigated pharmaceuticals and consequently, results on k_{photo} and k_{att} agreed rather well. To go deeper in our understanding of phototransformation mechanisms, TPs identification by LC-HRMS in irradiated Fe^{3+}/Cu^{2+} systems was suitable and highlighted specific and new transformation pathways including reductive transformation pathways due to dehalogenation and hydrogenation reactions. Their significance was confirmed by the detection of few of these TPs along the investigated river.

Acknowledgements

This research was supported by the EU PRIMA program through the research project INWAT – Quality and management of intermittent river and groundwater in Mediterranean basins. The authors thank the Platform of Non-Target Environmental Metabolomics (PONTEM) of the consortium facilities Montpellier Alliance for Metabolomics and Metabolism Analysis (MAMMA). Ecole des Mines d'Alès is thanked for the help in field sampling.

References

Alturiqi, A., 2018. Equilibrium studies of ternary complexes of Cu(II) with venlafaxine hydrochloride drug and some amino acids. Orient. J. Chem. 34, 580-585. http://dx.doi.org/10.13005/ojc/340170.

Alvarez, D., 2010. Guidelines for the use of the semipermeable membrane device (SPMD) and the polar organic chemical integrative sampler (POCIS) in environmental monitoring studies. USGS report. Tech. Methods 1–D4. 38 p. https://doi.org/10.3133/tm1D4.

Asif, A., Wang, S. Sun, H., 2021. Hematite-based nanomaterials for photocatalytic degradation of pharmaceuticals and personal care products (PPCPs): A short review. Curr. Opin. Green Sustain. Chem. 28, 100447. https://doi.org/10.1016/j.cogsc.2021.100447.

Baumanis, C., Bloh, J., Dillert, R., Bahnemann, D., 2011. Hematite photocatalysis: dechlorination of 2,6-dichloroindophenol and oxidation of water. J. Phys. Chem. C 115, 25442-2550. https://doi.org/10.1021/jp210279r.

Boukhalfaa, C., Reinertb, L., Duclaux, L., 2010. Copper coprecipitation with hydrous iron oxide in aqueous solutions: Spectroscopic, thermal and macroscopic analyses. Desalination and Water Treat. 18, 12-16. https://doi.org/10.5004/dwt.2010.1260.

490 Calisto, V., Domingues, R., Esteves, V., 2011. Photodegradation of psychiatric pharmaceuticals in
491 aquatic environments: kinetics and photodegradation products. Water Res., 4, 6045-6106.
492 https://doi.org/10.1016/j.watres.2011.09.008.

493 Castro G., Casado J, Rodríguez I., Ramil M., Ferradas A., Cela R., 2016. Time-of-flight mass
494 spectrometry assessment of fluconazole and climbazole UV and UV/H2O2 degradability: Kinetics
495 study and transformation products elucidation. Water Res., 88, 681-690.
496 http://dx.doi.org/10.1016/j.watres.2015.10.053.

497 Correia dos Santos M.M., Vila Famila, M.L. Gonçalves S., 2002. Copper–Psychoactive Drug
498 Complexes: A Voltammetric Approach to Complexation by 1,4-Benzodiazepines. Anal. Biochem., 303,
499 2, 111-119. https://doi.org/10.1006/abio.2002.5580.

500 El Azzi, D., Viers, J., Guiresse, M., Probst, A., Aubert, D., Caparros, J., Charles, F., Guizien, K., Probst, J-
501 L., 2013. Origin and fate of copper in a small Mediterranean vineyard catchment: New insights from
502 combined chemical extraction and δ65Cu isotopic composition. Sci. Total Environ., 463-464, 91-101.
503 http://dx.doi.org/10.1016/j.scitotenv.2013.05.058.

504 European Commission 2017. SANTE/11813/2017. Guidance document on analytical quality control
505 and method validation procedures for pesticides residues analysis in food and feed.
506 SANTE/11813/2017. *Eur Comm Dir Heal Food Saf*, 1-46.

507 Gornik, T., Carena, L., Kosjek, T. Vione, D., 2021. Phototransformation study of the antidepressant
508 paroxetine in surface waters. Sci. Total Environ., 774, 145380.
509 https://doi.org/10.1016/j.scitotenv.2021.145380.

510 Iles, J., Pettit, N., Donn, M., Grierson, P., 2022. Phosphorus sorption characteristics and interactions
511 with leaf litter-derived dissolved organic matter leachate in iron-rich sediments of a sub-tropical
512 ephemeral stream. Aquatic Sci. 84, 56. https://doi.org/10.1007/s00027-022-00888-x.

513 Jaeger, A., Posselt, M., Betterle, A., Schaper, J., Mechelke, J., Coll, C., Lewandowski, J., 2019. Spatial
514 and temporal variability in attenuation of polar organic micropollutants in an urban lowland stream.
515 Environ. Sci. Technol. 53, 2383-2395. http://dx.doi.org/10.1021/acs.est.8b05488.

516 Joseph S., Visalakshi G., Venkateswaran G., Moorthy P. N., 1995. Dissolution of Haematite in Citric
517 Acid-EDTA- Ascorbic Acid Mixtures. J. Nuclear Sci. Technol., 33:6, 479-485.
518 https://doi.org/10.1080/18811248.1996.9731940.

519 Kunkel, U., Radke, M., 2012. Fate of pharmaceuticals in rivers: Deriving a benchmark dataset at
520 favor.able attenuation conditions. Water Res., 46, 5551-5565.
521 https://doi.org/10.1016/j.watres.2012.07.033.

522 Lapshin, S., Alekseev, V., 2009. Copper(II) complexation with ampicillin, amoxicillin, and cephalexin.
523 Russian J. Inorg. Chem., 54, 1066-1069. DOI: https://doi.org/10.1134/S0036023609070122.

524 Lei, M., Wang, N., Zhub, L., Zhoub, Q., Niea, G., Tang, H., 2016. Photocatalytic reductive degradation
525 of polybrominated diphenyl ethers on CuO/TiO2 nanocomposites: A mechanism based on the
526 switching of photocatalytic reduction potential being controlled by the valence state of copper. Appl.
527 Catal. B : Environ. 182, 414-423. https://doi.org/10.1016/j.apcatb.2015.09.031.

528 Li, Z., Gomez, E., Fenet, H., Chiron, S., 2013. Chiral signature of venlafaxine as a marker of biological
529 attenuation processes. Chemosphere, 90, 1933-1938.
530 https://doi.org/10.1016/j.chemosphere.2012.10.033.

531 Li, Z., Sobek, A., Radke, M., 2015. Flume experiments to investigate the environmental fate of
532 pharmaceuticals and their transformation products in streams. Environ. Sci. Technol., 49, 6009-6017.
533 http://dx.doi.org/10.1021/acs.est.5b00273.

534 Li, Z., Sobek, A., Radke, M., 2016. Fate of phamaceuticals and their transformation products in four
535 small european rivers receiving treated wastewater. Environ. Sci. Technol. 50, 5614-5621.
536 http://dx.doi.org/10.1021/acs.est.5b06327.

537 Manasfi, R., D. Tadić, D., Gomez, O., Perez′ S., Chiron, S., 2022. Persistence of N-oxides
538 transformation products of tertiary amine drugs at lab and field studies. Chemosphere 309 Part 1,
539 136661. https://doi.org/10.1016/j.chemosphere.2022.136661.

540 Mandaric, L., Kalogianni, E., Skoulikidis, N., Petrovic, M., Sabater, S., 2019. Contamination patterns
541 and attenuation of pharmaceuticals in a temporary Mediterranean river. Sci. Total Environ. 647, 561-
542 569. https://doi.org/10.1016/j.scitotenv.2018.07.308.

543 Mansoor, F., Farooqui, M., 2017. Determination of pK and Log K values of tramadol hydrochloride
544 with Cu(II), Co(II) and Fe(II) metal ions. Intern. J. Appl. Res. 3(9), 385-386.
545 https://dx.doi.org/10.22271/allresearch.

546 Mechelke, J., Rust, D., Jaeger, A., Hollender, J., 2020. Enantiomeric fractionation during
547 biotransformation of chiral pharmaceuticals in recirculating water-sediment test flumes. Environ. Sci.
548 Technol. 54, 7291−7301. https://doi.org/10.1021/acs.est.0c00767.

549 Nakanishi, K., Yagi, R., Imamura, K., Tanaka, A., Hashimato, K., Kominami, H., 2018. Ring hydrogenation of
550 aromatic compounds in aqueous suspensions of an Rh-loaded TiO_2 photocatalyst without use of H_2 gas. Catal.
551 Sci. Technol. 8, 139-146. https://doi.org/10.1039/C7CY01929G.

552 Osawa R., Barrocas B. T., Monteiro O.C., Oliveira M. C., Florêncio M. H., 2019. Photocatalytic degradation of
553 amitriptyline, trazodone and venlafaxine using modified cobalt-titanate nanowires under UV–Vis radiation:
554 Transformation products and in silico toxicity. Chem. Engin. J. 373, 1338-1347.
555 https://doi.org/10.1016/j.cej.2019.05.137.

556 Pacholak, A., Burlaga, N., Frankowski, R., Zgola-Grzeskowiak, A., Kaczorek, E., 2022. Azole fungicides:
557 (Bio)degradation, transformation products and toxicity elucidation. Sci. Total Environ. 802, 149917.
558 https://doi.org/10.1016/j.scitotenv.2021.149917.

559 Perontsis, S., Hatzidimitriou, A., Begou, O-A, Papadopoulos, A., Psomas, G., 2016. Characterization
560 and biological properties of copper(II)-ketoprofen complexes. J. Inorg. Chem. 162, 22-30.
561 http://dx.doi.org/10.1016/j.jinorgbio.2016.06.001.

562 Redshaw, C., Cooke, M., Talbot, H., McGrath, S., Rowland, S., 2008. Low biodegradability of
563 fluoxetine HCl, diazepam and their human metabolites in sewage sludge-amended soil. J. Soils Sed. 8
564 (4), 217−230. https://doi.org/10.1007/s11368-008-0024-2.

565 Rua-Gomez, P., Püttmann, W., 2013. Degradation of lidocaine, tramadol, venlafaxine and the
566 metabolites *O*-desmethyltramadol – *O*-desmethylvenlafaxine in surface waters. Chemosphere, 90,
567 1952-1959. https://doi.org/10.1016/j.chemosphere.2012.10.039.

568 Schmitt, M., Wack, K., Glaser, C., Wei, R., Zwiener, C., 2021. Separation of photochemical and non-
569 photochemical diurnal in stream attenuation of micropollutants. Environ. Sci. Technol. 55, 8908-
570 8917. https://doi.org/10.1021/acs.est.1c02116.

571 Sibhatu, A., Weldegebrieal, G., Sagadevan, S., Tran, N., Hessel, V., 2022. Photocatalytic activity of CuO
572 nanoparticles for organic and inorganic pollutants removal in wastewater remediation. Chemosphere
573 300, 134623. https://doi.org/10.1016/j.chemosphere.2022.134623.

574 Simoes-Gonçalvez, M., Famila, V., Correja dos santos, M., 2002. Copper–psychoactive drug
575 complexes: A voltammetric approach to complexation by 1,4-benzodiazepines. Anal. Biochem. 303,
576 111-119. https://doi.org/10.1006/abio.2002.5580.

577 Stevanović, N., Aleksic, I., Kljun, J.,Bogojevic, S., Veselinovic, A., Nikodinovic-Runic, J., Turel, I., Djuran,
578 M,; Gliši c, B., 2021. Copper(II) and Zinc(II) complexes with the clinically used fluconazole:

579 Comparison of antifungal activity and therapeutic potential. Pharmaceuticals, 14, 24.
580 https://doi.org/10.3390/ph14010024.

581 Sun, L., Chen, H., Abdulla, H., Mopper, K., 2014. Estimating hydroxyl radical photochemical formation
582 rates in natural waters during long-term laboratory irradiation experiments. Environ. Sci. Process
583 Impacts 16, 757-763. https://doi.org/10.1039/c3em00587a.

584 Sykora, J., 1997. Photochemistry of copper complexes and their environmental aspects. Coord.
585 Chem. Rev., 159, 95-108. https://doi.org/10.1016/S0010-8545(96)01299-4.

586 Tadić, D., Manasfi, R., Bertrand, M., Sauvêtre, A., Chiron, S., 2022. Use of passive and grab sampling
587 and high-resolution mass spectrometry for non-targeted analysis of emerging contaminants and their
588 semi-quantification in water. Molecules, 27, 3167. https://doi.org/10.3390/molecules27103167.

589 West, C. and Rowland, S., 2012. Aqueous phototransformation of diazepam and related human
590 metabolites under simulated sunlight. Environ. Sci. Technol. 46, 4749-4756.
591 https://doi.org/10.1021/es203529z.

592 Xue, H., Sigg, L., Gächter, R., 2000. Transport of Cu, Zn and Cd in a small agricultural catchment.
593 Water Res., 34, 22558-2568. https://doi.org/10.1016/S0043-1354(00)00015-4.

594 Yang B., Xu C., Kookana R.S., Williams M., Du J., Ying G., Gu F., 2018. Aqueous chlorination of
595 benzodiazepines diazepam and oxazepam: Kinetics, transformation products and reaction pathways.
596 Chem. Engin. J. 354, 1100-1109. https://doi.org/10.1016/j.cej.2018.08.082.

597 Yu, Y., Xu, W., Chen, D., Fang, J., Zhu, X., Sun, J., Liang, Y., Hu, X., Li, R., Fang, Z., 2021. Adsorption-
598 photocatalysis synergistic removal of contaminants under antibiotic and Cr(VI) coexistence
599 environment using non-metal g-C_3N_4 based nanomaterial obtained by supramolecular self-assembly
600 method. J. Hazard. Mater. 404 Part A 124171. https://doi.org/10.1016/j.jhazmat.2020.124171.

Zhang X., Guo Y., Pan Y., 2020. Yang X. Distinct effects of copper on the degradation of β-lactam antibiotics in fulvic acid solutions during light and dark cycle. Environ. Sci. Technol. 3, 100051. https://doi.org/10.1016/j.ese.2020.100051.

Zhi, H., Kolpin, D., Klaper, D., Iwanowicz, L., Meppelink, S., Lefevre, G., 2020. Occurrence and spatiotemporal dynamics of pharmaceuticals in a temperate-region wastewater effluent-dominated stream: Variable inputs and differential attenuation yield evolving complex exposure. Environ. Sci. Technol. 54, 12967-12978. https://dx.doi.org/10.1021/acs.est.0c02328.

Zhi, H., Mianecki, A., Kolpin, D., Klaper, D., Iwanowicz, L., Lefevre, G., 2021. Tandem field and laboratory approaches to quantify attenuation mechanisms of pharmaceutical and pharmaceutical transformation products in a wastewater effluent-dominated stream. Water Res. 203, 117537. https://doi.org/10.1016/j.watres.2021.117537.

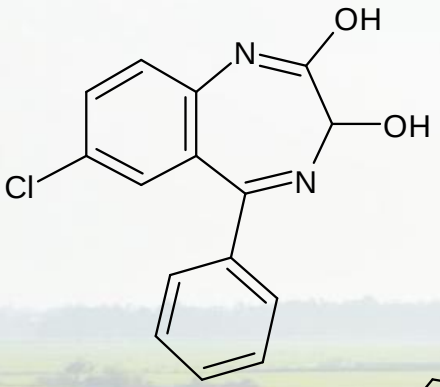

Oxazepam

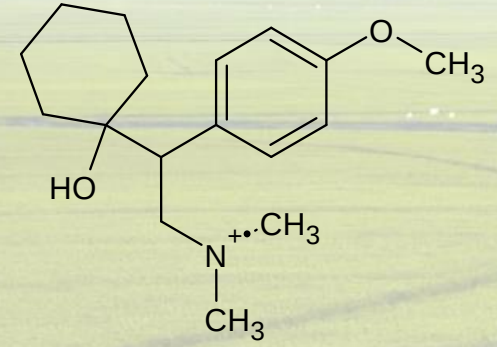

Venlafaxine

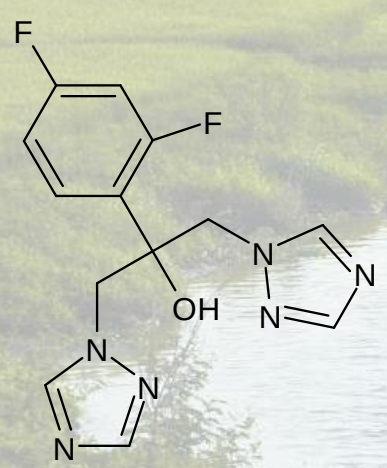

Fluconazole

Fe

Cu

Fe- and Cu-rich Mediterranean intermittent river

Photocatalytic redox transformation
dehalogenation, hydrogenation

10 TPs CONFIRMED IN RIVER SAMPLES

→ *in-stream attenuation of pharmaceuticals*

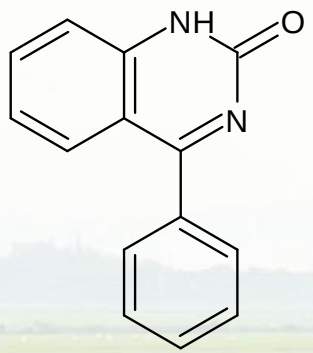

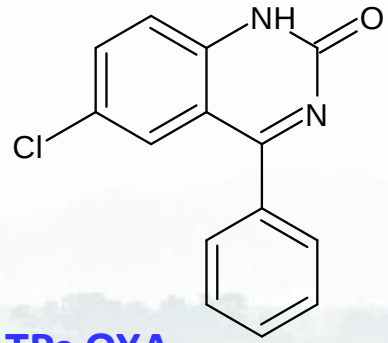

5 TPs OXA

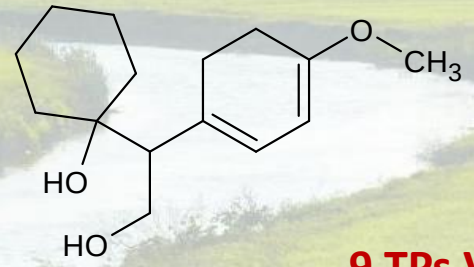

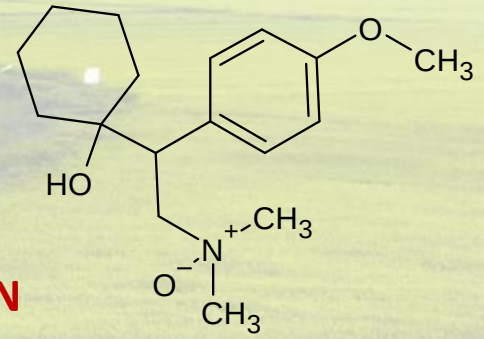

9 TPs VEN

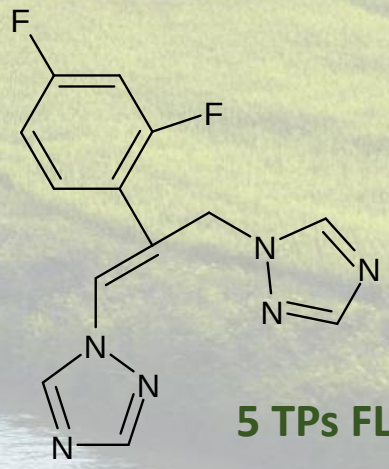

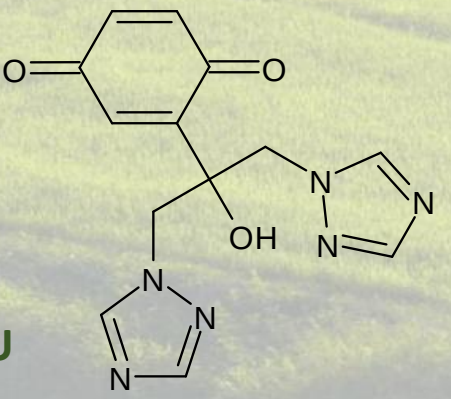

5 TPs FLU